Bioorganic & Medicinal Chemistry 23 (2015) 703–711

Contents lists available at ScienceDirect

Bioorganic & Medicinal Chemistry

journal homepage: www.elsevier.com/locate/bmc

Synthesis and anticancer cell potential of steroidal 16,17-seco-16,17a-dinitriles: Identification of a selective inhibitor of hormone-independent breast cancer cells

Andrea R. Nikolić [a,*], Edward T. Petri [b,*], Olivera R. Klisurić [c], Andjelka S. Ćelić [b], Dimitar S. Jakimov [d], Evgenija A. Djurendić [a], Katarina M. Penov Gaši [a], Marija N. Sakač [a]

[a] Department of Chemistry, Biochemistry and Environmental Protection, Faculty of Sciences, University of Novi Sad, Trg Dositeja Obradovića 3, 21000 Novi Sad, Serbia
[b] Department of Biology and Ecology, Faculty of Sciences, University of Novi Sad, Trg Dositeja Obradovića 2, 21000 Novi Sad, Serbia
[c] Department of Physics, Faculty of Sciences, University of Novi Sad, Trg Dositeja Obradovića 4, 21000 Novi Sad, Serbia
[d] Oncology Institute of Vojvodina, Institutski put 4, 21204 Novi Sad, Serbia

ARTICLE INFO

Article history:
Received 28 October 2014
Revised 26 December 2014
Accepted 29 December 2014
Available online 6 January 2015

Keywords:
Steroid
Nitrile
Breast cancer
Hormone-independent breast cancer
Molecular docking
Ligand-based screening

ABSTRACT

We report the synthesis of steroidal 16,17-seco-16,17a-dinitriles and investigate their antitumor cell properties. Compounds were evaluated for anticancer potential by in vitro antiproliferation studies, molecular docking and virtual screening. Several compounds inhibit the growth of breast and prostate cancer cell lines (MCF-7, MDA-MB-231 and PC3), and/or cervical cancer cells (HeLa). Supporting this, molecular docking predicts that steroidal 16,17-seco-16,17a-dinitriles could bind with high affinity to multiple molecular targets of breast and prostate cancer treatment (aromatase, estrogen receptor α, androgen receptor and 17α-hydroxylase) facilitated by D-seco flexibility and nitrile-mediated contacts. Thus, 16,17-seco-16,17a-dinitriles may be useful for the design of inhibitors of multiple steroidogenesis pathways. Strikingly, **10**, a 1,4-dien-3-on derivative, displayed selective submicromolar antiproliferative activity against hormone-dependent (MCF-7) and -independent (MDA-MB-231) breast cancer cells (IC_{50} 0.52, 0.11 μM, respectively). Ligand-based 3D similarity searches suggest AKR1C, 17β-HSD and/or 3β-HSD subfamilies as responsible for this antiproliferative activity, while fast molecular docking identified AKR1C and ERβ as potential binders-both targets in the treatment of hormone-independent breast cancers.

1. Introduction

Steroidal compounds serve as ligands or substrates for hormone receptors and steroidogenic enzymes in numerous biological processes, including cell growth and proliferation.[1] Hormonal steroids and metabolites influence the proliferation of hormone-responsive (e.g., ovarian, prostate, endometrial and breast) and other cancers (e.g., cervical and colorectal).[2–6] Thus, attenuation of circulating sex hormone levels is an important therapeutic strategy, and the development of selective antitumor compounds is a major goal of synthetic chemistry.[1] Anticancer drugs in clinical use against breast or prostate cancer include formestane (**I**), anastrozole (**II**), letrozole (**III**), and abiraterone (**IV**) (Fig. 1): which slow cancer growth in part by inhibiting steroidogenic cytochrome P450 enzymes, CYP19 (**I**–**III**) or CYP17 (**IV**). While **I** mimics steroidal CYP19 ligands[7], compounds **II**–**IV** also function by coordinating with the heme moiety in the active site of CYP19[8] or CYP17.[9] Other steroidal drugs (e.g., fulvestrant, megestrol and cyproterone) target hormone receptors, such as estrogen receptor α (ERα) and androgen receptor (AR).[10–12] Newer dinitrile containing non-steroidal CYP19 inhibitors (**II** and **III**) display enhanced oral bioavailability with reduced side effects, and are used to treat hormone receptor-positive (ER+) breast cancers in postmenopausal women.[13,14] However, because of the prevalence of cancers resistant to current treatments, the synthesis of steroid-based compounds with improved anticancer properties remains an active field of research.[1,15]

Nitrile modifications are often employed to enhance the physico-chemical properties of biologically active compounds, and can improve solubility (hydrophilicity), pharmacokinetics, and ADME toxicity profiles.[16] Pharmacologically, nitriles serve as bioisosteres of carbonyls, carboxyls, hydroxyls and halogens. In protein–ligand complexes, nitriles act as hydrogen bond acceptors,

* Corresponding authors. Tel.: +381 21 485 2772; fax: +381 21 454 065.
E-mail addresses: andrea.nikolic@dh.uns.ac.rs (A.R. Nikolić), edward.petri@dbe.uns.ac.rs (E.T. Petri).

http://dx.doi.org/10.1016/j.bmc.2014.12.069
0968-0896/

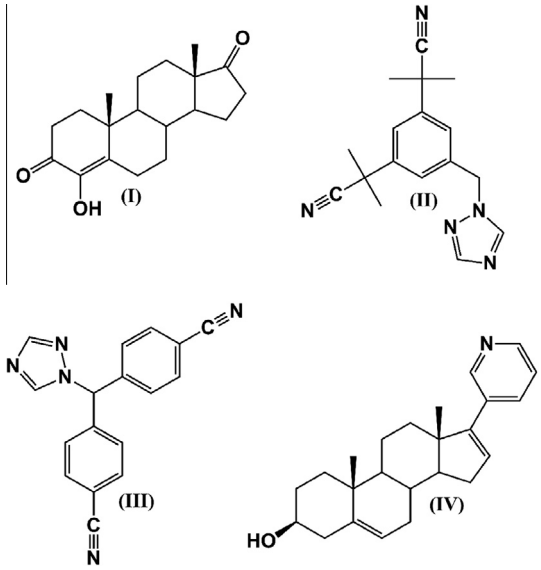

Figure 1. Selected anticancer drugs used in the treatment of breast or prostate cancer: formestane (**I**), anastrozole (**II**), letrozole (**III**), and abiraterone (**IV**).

and form non-specific dipole interactions with protein side chains or metal ions; where their short, linear geometry enables penetration into sterically-occluded protein pockets.[17] In fact, over 50 nitrile-containing drugs are in clinical use or under clinical evaluation.[16] For example, the steroidal drug trilostane (4α,5α-epoxy-3,17β-dihydroxyandrost-2-ene-2-carbonitrile) inhibits 3β-hydrox ysteroid dehydrogenase (an enzyme involved in breast cancer and conversion of DHEA to estradiol) through a critical nitrile–serine interaction;[18] while nitrile groups in **II** participate in CYP19 heme coordination.[8] We previously synthesized 16,17-secoandrost-5-ene-16-nitriles with antiproliferative activity against PC3 prostate cancer cells and both ER+ (MCF-7) and ER− (MDA-MB-231) breast adenocarcinomas.[19–21] In addition, steroidal D-ring carbonitriles with unsaturated A- or B-rings have been synthesized as possible CYP19 inhibitors.[22] Furthermore, C-17 nitrile-substituted estratrienes have been reported with strong antiproliferative activity against ER+ (MCF-7) breast cancer cells, and act as microtubule disruptors.[23] Given the potency of dinitrile-containing CYP19 inhibitors (e.g., **II**–**III**) and the anticancer potential of nitrile-modified steroidal drugs, we became interested in the synthesis and characterization of novel dinitrile-modified steroidal compounds for possible use in the development of more effective cancer therapeutics.

Here we present an efficient route for the preparation of new steroidal 16,17-seco-16,17a-dinitriles. Synthesized compounds were validated by X-ray crystallography and spectroscopy (IR, ^{1}H NMR, ^{13}C NMR, HRMS), and evaluated for anticancer potential by in silico molecular docking, ligand-based virtual screening, and in vitro antiproliferation studies. The influence of modified A-ring systems, such as 4-en-3-one, 4-en-4-ol-3-one, 1,4-dien-3-one, or an aromatic A-ring, was investigated. Molecular docking simulations were conducted against several targets of steroidal chemotherapeutic agents in clinical use for breast and prostate cancer treatment: Aromatase (CYP19A1), 17α-hydroxylase/17,20-lyase (CYP17A1), androgen receptor (AR) and estrogen receptor α (ERα). Antiproliferative activity was measured in vitro against seven human cancer cell lines: estrogen receptor negative (ER−) breast adenocarcinoma (MDA-MB-231); estrogen receptor positive (ER+) breast adenocarcinoma (MCF-7); prostate cancer (PC3); human cervical carcinoma (HeLa); myelogenous leukaemia (K562); A549 lung adenocarcinoma and colon adenocarcinoma

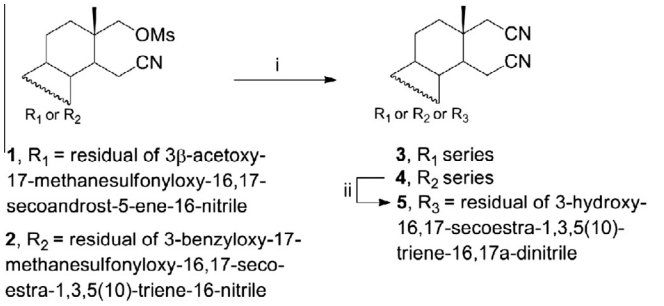

Scheme 1. Reagents and conditions: (i) NaCN, DMSO, reflux, 7.5 h; (ii) 10% Pd/C, dichloromethane, rt, 48 h.

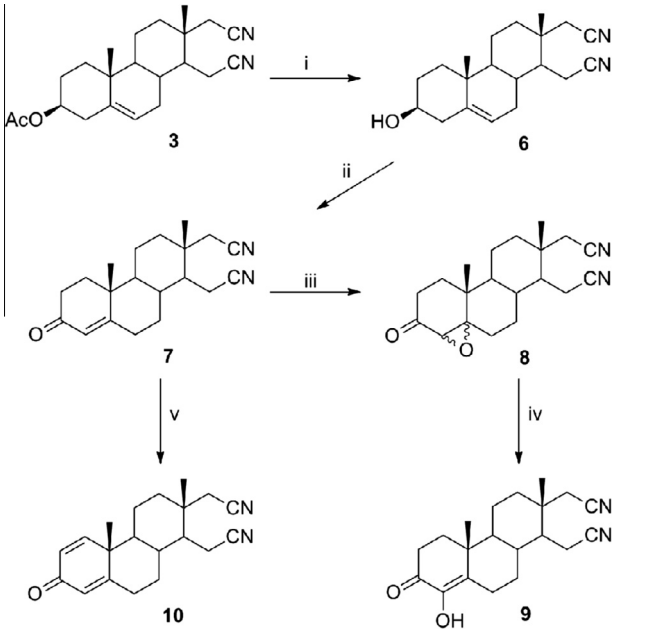

Scheme 2. Reagents and conditions: (i) EtONa, EtOH, 55 °C, 1 h; (ii) Al(*i*-PrO)$_3$, cyclohexanone, toluene, distillation, 4 h; (iii) H_2O_2, NaOH, MeOH, −15 °C, 90 min; (iv) HCOOH, reflux, 1 h; (v) DDQ, TFA, BSTFA, toluene, reflux, 6 h.

(HT-29); versus a normal non-cancerous control cell line (MRC-5). Ligand-based virtual screening (3D similarity and Protein Data Bank screening) was conducted to suggest a molecular basis for some cytotoxicity results.[24]

2. Results and discussion

2.1. Synthesis of new steroidal 16,17-seco-16,17a-dinitriles

To enable investigation of the anti-tumor cell potential of dinitrile-modified steroidal compounds, we developed a synthetic route for the preparation of new steroidal D-seco dinitriles from androstane and estrane mesylate **1** or **2**, which were prepared as described in our previous work.[20] The corresponding 16,17-seco-16,17a-dinitriles **3** or **4** were synthesized via substitution of the mesyloxy group in **1** or **2** with sodium cyanide in dimethyl sulfoxide (Scheme 1). Hydrogenolysis of benzyl ether **4** in the presence of 10% Pd/C resulted in 3-hydroxy derivative **5**. Treatment of compound **3** with sodium ethoxide in ethanol for 1 h afforded 3β-hydroxy derivative **6** (Scheme 2). Oppenauer oxidation of compound **6** was conducted using aluminum isopropoxide in a cyclohexanone–toluene system, to afford 4-en-3-one derivative **7**. Epoxidation of **7** with 30% H_2O_2 and an aqueous solution of sodium

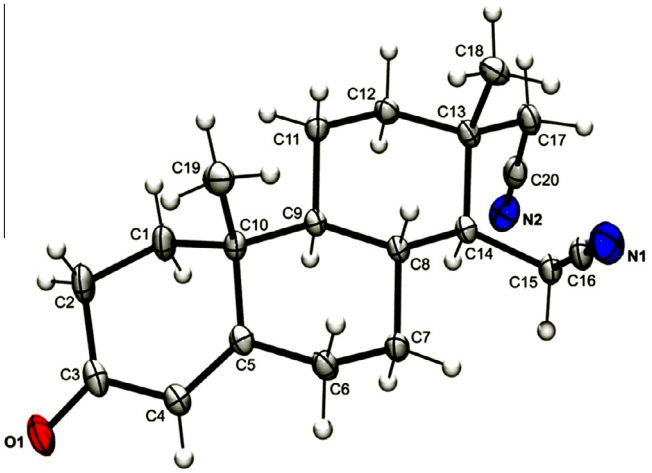

Figure 2. X-ray crystal structure of compound **7** (3-oxo-16,17-secoandrost-4-ene-16,17a-dinitrile). ORTEP drawing of the molecular structure of compound **7** with labeled non-H/non-C atoms. Displacement ellipsoids are shown at 50% probability, and H atoms are drawn as spheres of arbitrary radii.

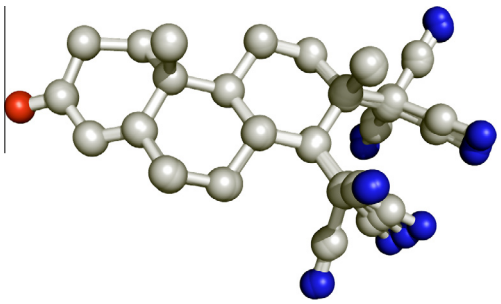

Figure 3. Conformer analysis of compound **7**. Superposition of energetically equivalent conformers of **7** identified by systematic rotomer search (energy range 282–309 kJ/mol; average 294 kJ/mol). Each nitrile group has a predicted partial electric charge of −0.197.

hydroxide in methanol (−15 °C for 90 min) resulted in a mixture of 4α,5α- and 4β,5β-epoxy derivatives **8a** and **8b**, which could not be separated. Opening of the oxirane ring in compounds **8a** and **8b** was performed with formic acid under reflux affording the corresponding 4-en-4-ol-3-on derivative **9**. The double bond at Δ^1 was introduced in **7** with 2,3-dichloro-5,6-dicyano-1,4-benzoquinone (DDQ) in toluene in the presence of trifluoroacetic acid (TFA) and bis(trimethylsilyl)trifluoroacetamide (BSTFA), following Marcos-Escribano et al. 2009, resulting in 1,4-dien-3-on derivative **10**.[25]

2.2. Structural and conformational analysis of steroidal 16,17-seco-16,17a-dinitriles

Compounds **5**–**10** were characterized by spectroscopy (IR, ^{1}H NMR, ^{13}C NMR) and HRMS (Supplemental S1). The three-dimensional structure of **7** was established by X-ray crystallography (data deposited at the Cambridge Crystallographic Data Centre; CCDC XXX) (Fig. 2) and used to create models of **5**–**10** (Supplemental S2 and S3). To obtain insight into the dynamics of steroidal 16,17-seco-16,17a-dinitriles, conformer analysis was conducted on **7** using a systematic rotor search in the program Avogadro; suggesting that the dinitrile modification can assume multiple conformations of approximately equal energy (Fig. 3).[26] *c*Log*P* calculations indicate that dinitrile modifications could improve the solubility of the steroid scaffold (*c*log*P* 2.06–2.80 for **5**–**10**), while **5**–**10** have calculated topological polar surface areas (TPSA) associated with high cell permeability (TPSA <140 Å^2), an important drug property (Table 1).[27]

Table 1
Predicted solubility (*c*log*P*) and cell permeability (topological polar surface area/TPSA) of compounds **5**–**10**

Compound	Energy (kJ/mol)	TPSA	*c*Log*P*
5	226.45	67.81	2.80
6	350.34	67.81	2.48
7	282.36	64.65	2.24
8a,**b**	315.57	77.18	2.06
9	327.13	84.88	2.16
10	306.63	64.65	2.60

*TPSA <140 Å^2 suggests a compound is cell permeable while TPSA <60 Å^2 suggests blood–brain barrier permeability.

Table 2
In vitro antiproliferative activities of A-ring modified steroidal 16,17-seco-16,17a-dinitriles **5**–**7**, **9**, **10**

Compound	HeLa	MDA MB-231	MCF-7	PC3	MRC-5[c]
5	7.32	3.96	16.96	11.18	>100
6	2.15	34.82	30.04	19.12	>100
7	5.73	15.51	15.02	8.27	>100
9	14.71	39.59	56.98	8.69	>100
10	12.49	**0.11**	**0.52**	70.85	>100
Formestane[a]	1.90	53.29	>100	45.65	>100
Doxorubicin[b]	1.17	0.12	0.75	95.61	0.12

IC_{50} (μM) values shown. IC_{50} values for **5**–**7**, **9**, **10** against HT-29, K562 and A560 cells were >100 μM and are not shown. Antiproliferative activity was determined using the MTT assay after exposure to 0.001, 0.01, 0.1, 1, 10 and 100 μM test compound for 48 h. Two independent experiments were conducted in quadruplicate for each concentration of test compound. Mean values and standard deviations (SD) were calculated for each concentration, and IC_{50} values were determined by median effect analysis.

[a] Control steroidal compound in clinical use against breast cancer.
[b] Control antiproliferative compound.
[c] Non-cancerous control.

2.3. In vitro antiproliferative activities of A-ring modified steroidal 16,17-seco-16,17a-dinitriles

As a preliminary test of the anti-cancer cell potential of D-seco dinitrile-modified steroids and the influence of various A-ring systems, **5**–**7**, **9** and **10** were evaluated for in vitro antiproliferative activity against a panel of human cancer cell lines: MCF-7 (human breast adenocarcinoma, ER+), MDA-MB-231 (human breast adenocarcinoma, ER−, triple-negative), PC3 (prostate cancer), HeLa (human cervical carcinoma), HT-29 (colon cancer) and A549 (human lung carcinoma), using the standard MTT assay.[28] Normal, non-cancerous cells (MRC-5 fetal lung fibroblasts) were used as a cytotoxicity control. Results were analyzed with respect to a non-selective cytotoxic drug (doxorubicin, DOX) and the steroidal CYP19/aromatase inhibitor formestane, which was included as a control for general steroidal toxicity (Table 2). Note that doxorubicin was highly toxic to non-cancerous MRC-5 cells, consistent with nonspecific cytotoxicity, but inactive against PC3 cells in agreement with previous reports.[29]

All of the tested compounds (**5**–**7**, **9** and **10**) displayed significant antiproliferative activity against cervical cancer cells (HeLa), with IC_{50} values ranging from 2.15 to 14.71 μM, suggesting a general role for 16,17-seco-16,17a-dinitrile modifications in HeLa cell growth inhibition. Interestingly, although formestane displayed strong antiproliferative activity against HeLa cervical cancer cells, combining the 16,17-seco-16,17a-dinitrile modification with the 4-en-4-ol-3-one system of formestane (compound **9**) somewhat reduced HeLa cell growth inhibition activity (formestane IC_{50}

1.90 μM vs compound **9** IC_{50} 14.71 μM); similar activity was observed with the 1,4-dien-3-on derivative (compound **10**, IC_{50} 12.49 μM). In contrast, the antiproliferative activities of **6** (IC_{50} 2.15 μM) and **7** (5.73 μM), with 5-en-3β-ol and 4-en-3-one systems, respectively, were comparable to formestane (IC_{50} 1.90 μM). Although the molecular mechanism of formestane (4-hydroxyandrost-4-ene-3,17-dione) inhibition of HeLa cell growth remains unclear, formestane is a known inhibitor of CYP19, as well as 5α-reductase and other enzymes involved in steroidogenesis and cell proliferation.[30,31] Other steroidal compounds modulate the proliferation of epithelial cervical cancer cells,[6] suggesting that **6** and **7** could have similar bioactivity, although further research is required.

Strong antiproliferative activity was found for nearly all compounds (except **10**) against prostate cancer cells (PC3), with compound **7** (IC_{50} 8.27 μM) again displaying significant activity. In fact, **5** and **7** inhibited the growth of four separate cancer cell lines (MCF-7, MDA-MB-231, PC3 and HeLa), suggesting that the conformational flexibility imparted by the 16,17-seco-16,17a-dinitrile modification enables interaction with multiple cellular targets (see Fig. 3). In particular, compound **5**, with an aromatic A-ring, was highly active against triple negative MDA-MB-231 breast cancer cells (IC_{50} 3.96 μM), but showed somewhat weaker activity against ER+ MCF-7 cells (IC_{50} 16.96 μM), suggesting a possible target(s) which is differentially expressed in ER− versus ER+ breast cancers.

Strikingly, compound **10**, with a 1,4-dien-3-one system, displayed selective submicromolar antiproliferative activity against ER− (MDA-MB-231) and ER+ (MCF-7) breast cancer cells (IC_{50} 0.11 and 0.52 μM, respectively) at levels comparable to doxorubicin controls (IC_{50} 0.12 and 0.75 μM, respectively). At a concentration of 10 nM, compound **10** inhibited 61% (MCF-7) and 69% (MDA-MB-231) of breast cancer cell growth (Fig. 4). In addition, in contrast with doxorubicin, **10** was nontoxic to most other cancer cell types (except HeLa cells where moderate activity was observed), and displayed no cytotoxicity against normal non-cancerous controls, indicating that this effect could be specific for breast cancer cells.

To begin to probe the molecular mechanisms behind this observed antiproliferative activity, we conducted a preliminary assessment of the apoptosis induction potential of **5**–**7**, **9** and **10** by visual inspection of treatment induced cell morphological changes in MDA-MB-231 breast cancer cells (Supplemental S4). Cells were treated with test compounds or controls at their respective antiproliferation IC_{50} concentrations (see Table 2). All test compounds displayed mild pro-apoptotic activity versus controls (11–18% apoptotic cells vs 7%, respectively). However, no dramatic increase in apoptosis associated morphological changes was observed under the current assay conditions. Because compound **10** displays submicromolar antiproliferative activity against MDA-MB-231 cells, it is possible that this antiproliferative activity represents growth arrest rather than apoptosis induction. However, detailed analysis of test compound induced changes to apoptotic and cell cycle pathways is clearly necessary. MDA-MB-231 breast adenocarcinoma cells are triple-negative; and triple-negative breast cancers are associated with poor patient prognosis. Since few targeted therapies have been developed to date for triple-negative breast cancers, identification of compounds such as **10** which inhibit the proliferation of MDA-MB-231 cell lines could be important for the future development of more effective therapies.

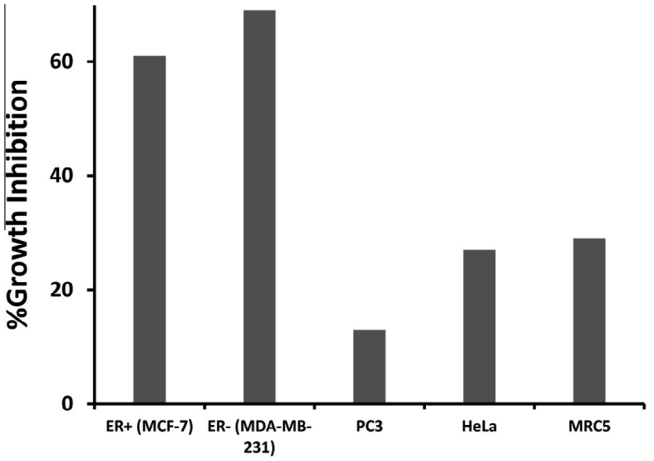

Figure 4. Growth inhibition (%) of hormone-dependent and independent breast cancer cell lines following treatment with 10 nM compound **10**.

2.4. Molecular docking of A-ring modified steroidal 16,17-seco-16,17a-dinitriles

To complement antiproliferative studies and suggest possible protein targets for A-ring modified steroidal 16,17-seco-16,17a-dinitriles, molecular docking simulations were conducted as described previously[28] on **5**–**7**, **9** and **10** against four protein targets of steroidal chemotherapeutic drugs used in the treatment of breast and prostate cancer: CYP17A1 (17α-hydroxylase/C17,20-lyase, PDB ID: 3RUK),[9] CYP19A1 (aromatase, PDB ID: 3EQM),[7] estrogen receptor (ERα, PDB ID: 1A52)[32] and androgen receptor (AR, PDB ID: 2AMA)[33] (Table 3). The X-ray structure of **7** was used as a template to model 3D ligand structures for docking (Supplemental S2). Docking was conducted using randomized initial coordinates and a maximal search space to minimize bias. High-throughput simulations were processed using the supercomputer cluster at the National Biomedical Computational Resource (http://nbcr-222.ucsd.edu/opal2), with the virtual screening tool PyRx,[34] and performed in Autodock.[35] Control docking simulations were conducted using ligands present in the X-ray crystal structures of the receptors. All control re-docking simulations reproduced ligand–protein geometries present in the respective crystal structures (RMSD ⩽ 0.6 Å, see[28]). Although no crystal structure of formestane has been solved in complex with its target CYP19, formestane is a well-known CYP19 inhibitor and was thus included for comparison in CYP19 docking simulations. Predicted binding energies approximately <−10 kcal/mol were considered significant based on control docking studies.

As can be seen in Table 3, compounds **5**, **7**, **9** and **10** are predicted to bind with significant affinity to more than one target, facilitated by the flexibility of the D-seco modification and the ability of nitriles to form polar contacts with multiple protein func-

Table 3
Molecular docking of **5**–**7**, **9** and **10** with protein targets of steroidal anti-cancer drugs: aromatase (CYP19), 17α-hydroxylase (CYP17), androgen receptor (AR) and estrogen receptor (ERα)

Compound	CYP19	CYP17	AR	ERα
5	−10.11	−9.44	−9.64	−10.53
6	−11.14	−10.46	−10.63	−11.17
7	−11.20	−10.11	−10.35	−10.36
9	−10.35	−10.45	−9.56	−9.45
10	−11.08	−10.09	−10.54	−10.31
ASD	−11.48			
Abiraterone		−11.66		
DHT			−10.99	
EST				−10.26
Formestane	−11.81[a]			

[a] Included for comparison.

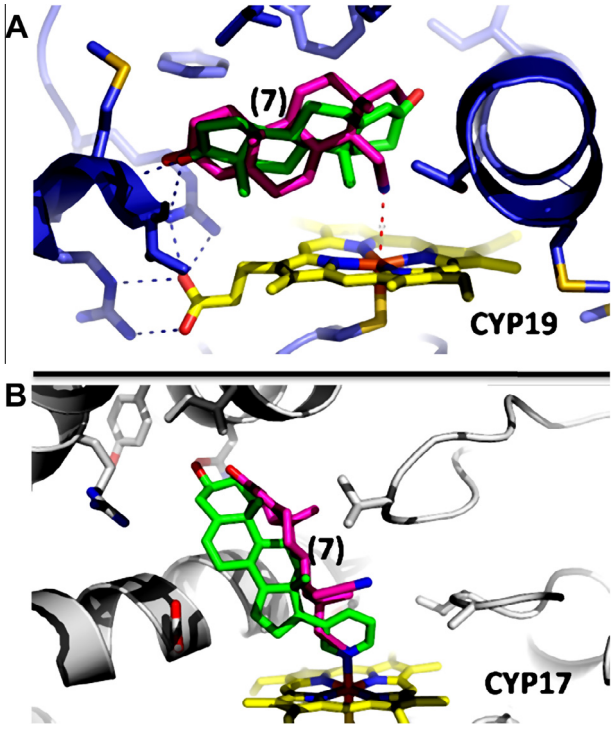

Figure 5. Molecular docking suggests that D-seco nitrile groups in 16,17-seco-16,17a-dinitrile steroidal compounds are capable of coordinating Heme Fe in CYP19 and CYP17. Compound **7** (magenta) is shown docked with X-ray structure of CYP19 (A) and CYP17 (B): androstenedione (panel A, CYP19) and the inhibitor abiraterone (panel B, CYP17) are shown in green for comparison.

Table 4
Predicted molecular targets for **10** based on 3D ligand similarity searches using ChemMapper3D and the DrugBank database

Protein	UniProt	Similarity	Score
Progesterone receptor	P06401	1.30	1
Mineralocorticoid receptor	P08235	1.30	1
Aldo keto reductase 1C1	Q04828	1.37	0.672
Estradiol 17β-dehydrogenase 1	P14061	1.49	0.667
Estrogen receptor α	P03372	1.29	0.604
3β-HSD/Δ5->4-isomerase	P14060	1.24	0.237

tional groups.[16] In fact, **6**, **7** and **10** are predicted to bind significantly to all four targets tested. These results suggest that 16,17-seco-16,17a-dinitriles may be useful scaffolds for the design of steroidal compounds which could inhibit more than one target involved in steroidogenesis. This strategy is currently being tested in clinical anticancer trials such as those investigating the use combined use of abiraterone (CYP17 inhibitor) and exemestane (CYP19 inhibitor) for the treatment of ER+ metastatic breast cancer (NCT01381874). Moreover, dual aromatase–steroid sulfatase inhibitors have shown promise in preclinical trials, while dual aromatase–aldosterone synthase inhibitors are in development.[36] Based on docking simulations, the D-seco modification could enable the nitrile group to coordinate directly with the heme Fe in both CYP17 and CYP19, a common property of inhibitors of cytochrome P450 enzymes (Fig. 5), including abiraterone (CYP17), letrozole and anastrozole (CYP19).

2.5. Ligand-based virtual screening to identify possible molecular targets of compound 10

Compound **10** displays submicromolar antiproliferative activity against ER+ and ER− breast cancer cell lines, but is not toxic to other tested cancer cell types (with the exception of HeLa cells) or a normal non-cancerous cell line, suggesting that this antiproliferative effect is specific for breast cancer cells. To propose possible molecular targets which may be responsible for the bioactivity of **10**, and to serve as a guide for future investigations, we conducted ligand-based virtual screening using two different approaches.

First we conducted a 3D similarity search using the program ChemMapper3D,[37] which assumes that small molecules with similar 2D or 3D structures have similar bioactivities and target proteins. ChemMapper3D screens test compounds against databases of chemical structures with associated bioactivities and target proteins. Compound **10** was screened against the DrugBank database, which contains 7739 drugs associated with 4283 non-redundant protein targets.[38,39] Predicted protein targets for **10** based on ChemMapper3D are shown in Table 4. Interestingly, all of the identified proteins are drug targets in the treatment of breast cancer. In particular, enzymes of the AKR1C, 17β-HSD and 3β-HSD subfamilies modify steroid hormones and have been implicated in the proliferation of hormone-dependent and/or hormone-independent human breast cancers.[40] In fact, AKR1C3 has been proposed as a drug target in the treatment of breast cancer, including triple negative breast cancers: small molecule inhibitors are in preclinical trials (see e.g., [41]).

Potential molecular targets for **10** were also proposed by rapid molecular docking against the entire protein data bank (PDB) using the program idTarget.[42] Proteins were considered possible targets of **10** if their predicted binding energy was >−9.5 kcal/mol with a *Z*-score of 1.0 or better. This preliminary list of 30 non-redundant proteins was further filtered by comparison with published reports of proteins expressed in hormone-dependent and -independent breast cancers, resulting in 8 putative candidates for interaction with **10** (see Table 5). As can be seen, there is significant overlap between proteins predicted by ChemMapper3D and idTarget, despite the use of very different algorithms. Importantly, two of the potential proteins, ERβand AKR1C3, are currently being investigated as drug targets in the treatment of hormone-independent breast cancers.[43–45] Predicted binding poses for **10** in complex with these 2 target proteins were analyzed in PyMol (Fig. 6). Interestingly, the crystal structure of ERβ identified by idTarget was solved in complex with a nitrile containing inhibitor (WAY-244).[45]

Table 5
Possible breast cancer associated protein targets for compound **10** identified by fast docking against the PDB database using idTarget

PDB	Protein	Binding energy (Δ*G*, kcal/mol)
3C3U	Aldo-keto reductase 1C1 AKR1C1	−10.20
1X78	Estrogen receptor β	−9.99
2Q8G	Pyruvate dehydrogenase kinase 1 PDK1	−9.93
1Y9R	Mineralocorticoid receptor	−9.90
1SR7	Progesterone receptor	−9.86
1M2Z	Glucocorticoid receptor	−9.81
2Q7I	Androgen receptor	−9.68
1RY0	Aldo-keto reductase 1C3 AKR1C3	−9.14

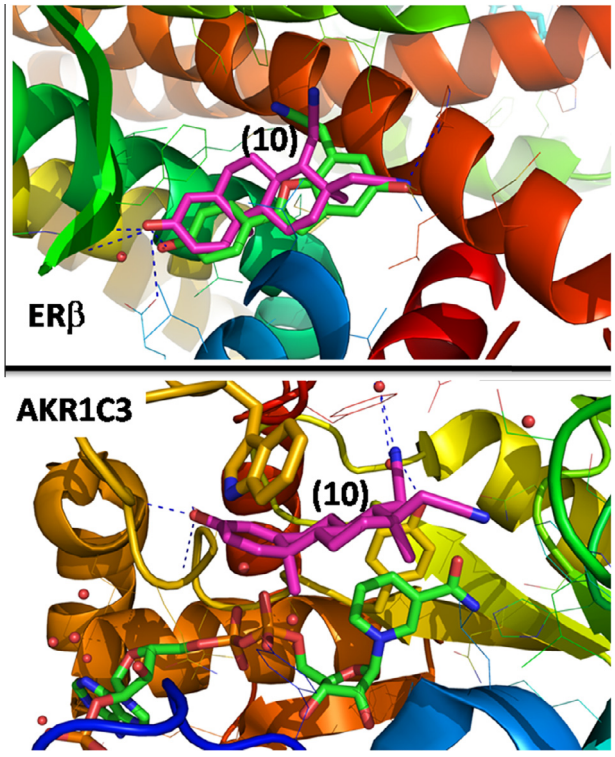

Figure 6. Visualization of idTarget fast docking results for compound **10** (magenta) docked with breast cancer drug targets ERβ (A) and AKR1C3 (B). ERβ is shown in complex with nitrile containing inhibitor WAY-244 (green).

Compound **10** is predicted to adopt a similar binding orientation with comparable hydrogen bonding, while one nitrile group from **10** occupies the same space as the nitrile in WAY-244. In ERα negative breast cancer patients, ERβ is considered to be a possible target for therapeutic intervention.[44] Similar analysis suggests that **10** could interact strongly with ARK1C family proteins, including ARK1C3. Because of the reported role of AKR1C family proteins (AKR1C3 in particular) in the growth and progression of hormone independent prostate and breast cancers, selective AKR1C inhibitors are currently under development.[46]

While results from ligand-based virtual screening are theoretical, the above methods have successfully identified drug targets for numerous compounds and have correctly predicted on and off-target modes of action for known drugs.[24] Given the strong, selective antiproliferative activity of compound **10** against breast cancer cell lines, additional research is warranted into its bioactivity and pharmacological potential; these ligand-based screening results are intended only as a guide for future research.

3. Conclusions

New steroidal 16,17-seco-16,17a-dinitriles were synthesized with potentially promising antitumor cell properties, particularly against breast cancer cell lines. Several compounds inhibit the growth of multiple cancer cell lines, in agreement with molecular docking results which predict that some steroidal 16,17-seco-16,17a-dinitriles could bind with high affinity to multiple molecular targets. Our results suggest that steroidal D-seco-16,17a-dinitriles may serve as flexible scaffolds for the design of compounds which modulate multiple steroidogenesis pathways. One compound, **10**, displayed submicromolar antiproliferative activity against both hormone-dependent and -independent breast cancer cells, with no toxicity to non-cancerous cells. Ligand-based 3D similarity and fast molecular docking screens were used to propose AKR1C and ERβ as molecular targets potentially responsible for this antiproliferative activity. These preliminary results require further investigation, especially considering the current difficulties associated with treating hormone-independent breast cancers.

4. Materials and methods

4.1. Chemical synthesis

4.1.1. General

IR spectra were measured on a NEXUS 670 SP-IR spectrometer (wave numbers in cm^{-1}). NMR spectra were recorded on a Bruker AC 250E spectrometer operating at 250 MHz (^1H) and 62.5 MHz (^{13}C), and are reported in ppm (δ-scale) downfield from the tetramethylsilane internal standard; coupling constants (J) are given in Hz. High resolution mass spectra (TOF) were recorded on a 6210 Time-of-Flight LC/MS Agilent Technologies (ESI+) instrument. Melting points were determined using an electrothermal 9100 apparatus and are reported uncorrected. Chromatographic separations were performed on silica gel columns (Kieselgel 60, 0.04–0.063 mm, Merck). All reagents used were of analytical grade. All solutions were dried over anhydrous sodium sulfate.

4.1.2. 3β-Acetoxy-16,17-secoandrost-5-ene-16,17a-dinitrile (3) and 3-(benzyloxy)-16,17-secoestra-1,3,5(10)-triene-16,17a-dinitrile (4)

To a solution of **1** or **2** (1 mmol) in dry dimethyl sulfoxide (5 mL), sodium cyanide (1.6 mmol) was added and the reaction mixture stirred at reflux for 7.5 h under a nitrogen atmosphere. After cooling, the reaction mixture was poured into a saturated solution of ammonium chloride (200 mL), and extracted with dichloromethane (3 × 20 mL). The combined organic extracts were dried and evaporated. The crude product was purified by column chromatography (toluene–ethyl acetate, 8:1 for **3**, or toluene–ethyl acetate, 10:1 for **4**) affording pure compound **3** or pure compound **4**.

3β-Acetoxy-16,17-secoandrost-5-ene-16,17a-dinitrile (3). White solid (63%, mp 166–169 °C after recrystallization from ethyl acetate). IR (KBr, cm^{-1}): 2943, 2909, 2856, 2237, 1734, 1723, 1247, 1030. ^1H NMR ($CDCl_3$, ppm): 1.05 (s, 3H, H-19); 1.15 (s, 3H, H-18); 2.05 (s, 3H, CH_3, Ac); 2.38 (s, 2H, H-17); 2.57 (dd, 1H, J_{gem} = 17.7 Hz, $J_{15a,14}$ = 5.5 Hz, H-15a); 4.61 (m, 1H, H-3); 5.39 (m, 1H, H-6). ^{13}C NMR ($CDCl_3$, ppm): 15.60 (C-15); 19.08; 19.12; 20.13; 21.41 (CH_3, Ac); 27.46; 31.09; 31.61; 31.98; 36.49; 36.65; 36.79; 37.59; 38.08; 45.82; 48.63; 73.43 (C-3); 117.10 (CN); 118.29 (CN); 120.97 (C-6); 139.39 (C-5); 170.54 (C=O, Ac). Anal. Calcd for $C_{22}H_{30}N_2O_2 \times 0.25H_2O$ (358.99): C, 73.60; H, 8.56; N, 7.84. Found: C, 73.82; H, 8.84; N, 7.93.

3-(Benzyloxy)-16,17-secoestra-1,3,5(10)-triene-16,17a-dinitrile (4). White solid (34%, mp 144 °C after recrystallization from *n*-hexane–acetone). IR (KBr, cm^{-1}): 3032, 2923, 2242, 1608, 1500, 1237, 1025. ^1H NMR ($CDCl_3$, ppm): 1.15 (s, 3H, H-18); 2.67 (dd, 1H, J_{gem} = 17.8 Hz, $J_{15a,14}$ = 5.4 Hz, H-15a); 5.06 (s, 2H, CH_2, Bn); 6.74–7.47 (group of signals, 8H, Ar H). ^{13}C NMR ($CDCl_3$, ppm): 15.87 (C-15); 19.06 (C-18); 26.07; 26.99; 29.79; 31.20; 37.03; 38.52; 39.46; 42.58; 44.34; 69.94 (CH_2, Bn); 112.77; 114.44; 117.12 (CN); 118.38 (CN); 126.33; 127.42; 127.88; 128.54; 131.28; 137.10; 137.28; 157.06 (C-3). HRMS (TOF) *m/z*: $C_{26}H_{28}N_2O$ $[M+H]^+$ calculated: 385.22744. Found: 385.22694.

4.1.3. 3-Hydroxy-16,17-secoestra-1,3,5(10)-triene-16,17a-dinitrile (5)

To a solution of **4** (47.8 mg, 0.16 mmol) in dichloromethane (2.5 mL) Pd/C (10%, 6.5 mg) was added and stirred vigorously

under a hydrogen atmosphere at room temperature for 24 h. Then, another portion of 10% Pd/C (4.9 mg) was added and the reaction mixture was stirred continuously for 24 h. When the reaction was complete, the resulting mixture was filtered to remove the catalyst and the filtrate evaporated. The precipitated solid product (35.7 mg, 98%), was recrystallized from dichloromethane–methanol, affording compound **5** in the form of white crystals.

Mp 222 °C. IR (KBr, cm^{-1}): 3344, 2944, 2921, 2254, 1611, 1508, 1446, 1230. ^1H NMR (acetone-d_6, ppm): 1.11 (s, 3H, H-18); 2.64 (dd, 1H, J_{gem} = 18.0 Hz, $J_{15a,14}$ = 3.9 Hz, H-15a); 6.56 (d, 1H, J = 2.4 Hz, H-4); 6.63 (dd, 1H, $J_{1,2}$ = 8.4 Hz, $J_{2,4}$ = 2.4 Hz, H-2); 7.14 (d, 1H, J = 8.4 Hz, H-1); 8.05 (s, 1H, OH). ^{13}C NMR (acetone-d_6, ppm): 16.01 (C-15); 18.68 (C-18); 27.02; 27.82; 30.50; 30.85; 37.56; 39.02; 41.12; 43.54; 45.54; 113.90; 115.65; 118.59 (CN); 120.17 (CN); 127.25; 131.07; 138.03; 156.24 (C-3). HRMS (TOF) m/z: $C_{19}H_{22}N_2O$ $[M+H]^+$ calculated: 295.18049. Found: 295.17978.

4.1.4. 3β-Hydroxy-16,17-secoandrost-5-ene-16,17a-dinitrile (6)

To a solution of sodium ethoxide in ethanol (0.1 M, 50 mL), compound **3** (1.16 g, 3.71 mmol) was added and the reaction mixture was heated to 55 °C with vigorous stirring for 1 h. Then, the mixture was poured into water (300 mL) and acidified (6 M HCl). The precipitated solid product (1.01 g, 99%), was recrystallized from ethyl acetate, affording compound **6** in the form of white crystals.

Mp 158–161 °C. IR (KBr, cm^{-1}): 3480, 2967, 2939, 2898, 2246, 1052. ^1H NMR ($CDCl_3$, ppm): 1.03 (s, 3H, H-19); 1.13 (s, 3H, H-18); 2.38 (s, 2H, H-17); 2.57 (dd, 1H, J_{gem} = 17.7 Hz, $J_{15a,14}$ = 5.5 Hz, H-15a); 3.53 (m, 1H, H-3); 5.36 (m, 1H, H-6). ^{13}C NMR ($CDCl_3$, ppm): 15.61 (C-15); 19.09; 19.20; 20.17; 31.05; 31.28; 31.62; 32.10; 36.64; 36.68; 36.73; 38.09; 41.70; 45.87; 48.72; 71.35 (C-3); 117.12 (CN); 118.37 (CN); 120.04 (C-6); 140.42 (C-5). HRMS (TOF) m/z: $C_{20}H_{28}N_2O$ $[M+Na]^+$ calculated: 335.20938. Found: 335.20906. Anal. Calcd for $C_{20}H_{28}N_2O \times 0.5H_2O$ (321.46): calculated C, 74.72; H, 9.09; N, 8.71. Found: C, 74.38; H, 9.31; N, 8.77.

4.1.5. 3-Oxo-16,17-secoandrost-4-ene-16,17a-dinitrile (7)

A solution of aluminum isopropoxide (1.39 g, 6.81 mmol) in dry toluene (35 mL) was added dropwise during azeotropic distillation to a solution of **6** (1.06 g, 3.41 mmol) in dry toluene (300 mL) and cyclohexanone (100 mL). The reaction mixture was heated for 4 h during azeotropic distillation. Then it was acidified (6 M HCl) and subjected to steam distillation. Upon distillation and cooling, the resulting product was extracted with dichloromethane (4 × 20 mL). The combined extracts were dried and the solvent removed. The crude product was purified by flash chromatography (toluene–ethyl acetate, 30:1) giving compound **7** in the form of a white solid (0.92 g, 87%, mp 128 °C after recrystallization from *n*-hexane–ethyl acetate).

IR (KBr, cm^{-1}): 2930, 2855, 2243, 1661, 1624, 1437, 1390, 1215, 735. ^1H NMR ($CDCl_3$, ppm): 1.17 (s, 3H); 1.22 (s, 3H); 2.62 (dd, 1H, J_{gem} = 18.0 Hz, $J_{15a,14}$ = 5.9 Hz, H-15a); 5.77 (s, 1H, H-4). ^{13}C NMR ($CDCl_3$, ppm): 15.80 (C-15); 17.50 (C-19); 19.09 (C-18); 20.28; 31.04; 31.15; 32.20; 33.75; 35.41; 35.77; 36.71; 38.29; 38.51; 44.87; 52.33; 116.87 (CN); 118.09 (CN); 124.08 (C-4); 168.68 (C-5); 198.93 (C-3). HRMS (TOF) m/z: $C_{20}H_{26}N_2O$ $[M+H]^+$ calculated: 311.21179. Found: 311.21204. Anal. Calcd for $C_{20}H_{26}N_2Ox0.1H_2O$ (312.43): C, 76.81; H, 8.39; N, 8.96. Found: C, 76.93; H, 8.39; N, 8.97.

4.1.6. 4α,5α- and 4β,5β-Epoxy-3-oxo-16,17-secoandrostane-16,17a-dinitrile (8a and 8b)

Hydrogen peroxide (30%, 0.4 mL, 0.35 mmol) and NaOH (0.1 M, 0.25 mL, 0.025 mmol) were added to **7** (0.1 g, 0.32 mmol) in methanol (3.6 mL), cooled to −15 °C, and the reaction mixture incubated at −15 °C for 90 min. The resulting reaction mixture was poured into water (100 mL), acidified with 6 M HCl and extracted with dichloromethane (3 × 20 mL). The combined extracts were dried and the solvent removed. Crude product was purified by column chromatography (14 g silica gel, toluene–ethyl acetate, 30:1), affording a mixture of 4α,5α- and 4β,5β-epoxy derivatives **8a** and **8b** (0.031 g, 30%) in the form of colorless oil.

IR (film, cm^{-1}): 3058, 2946, 2856, 2243, 1707, 1438, 1391, 1267, 861, 786, 736, 702. ^1H NMR ($CDCl_3$, ppm): 1.17 and 1.18 (2s, 3H, H-19); 1.20 (s, 3H, H-18); 2.58 and 2.65 (2dd, 1H, J_{gem} = 10.3 Hz, $J_{15a,14}$ = 5.8 Hz, H-15a); 3.04 and 3.11 (2s, 1H, H-4α and H-4β). ^{13}C NMR ($CDCl_3$, ppm): 15.80 and 15.91 (C-15); 16.55 (C-18); 18.83 and 19.14 (C-19); 20.68; 25.86; 29.06 and 29.18; 29.67 and 29.78; 31.04 and 31.16; 32.40; 32.85; 35.28 and 35.52; 38.24 and 38.34; 44.70 and 44.90; 45.34; 49.28; 62.33 and 62.58 (C-4); 69.01 and 69.29 (C-5); 116.84 and 116.92 (C-20, CN); 118.04 and 118.09 (C-16, CN); 205.75 and 206.05 (C-3). HRMS (TOF) m/z: $C_{20}H_{26}N_2O_2$ $[2M+H]^+$ calculated: 653.40613. Found: 653.40750.

4.1.7. 4-Hydroxy-3-oxo-16,17-secoandrost-4-ene-16,17a-dinitrile (9)

A mixture of epoxides **8a** and **8b** (68.3 mg, 0.21 mmol) was refluxed in formic acid (1 mL, 10 mmol) for 1 h. After cooling, the reaction mixture was poured into water (5 mL) and extracted with dichloromethane (3 × 5 mL). The combined extracts were dried and the solvent removed. Crude product was purified by flash chromatography (toluene–ethyl acetate, 2:1) affording compound **9** (28 mg, 41%, mp 129–130 °C after recrystallization from *n*-hexane–acetone) in the form of white solid.

IR (KBr, cm^{-1}): 3420, 2937, 2244, 1662, 1636, 1383, 1170. ^1H NMR ($CDCl_3$, ppm): 1.16 (s, 3H, H-19); 1.20 (s, 3H, H-18); 6.09 (s, 1H, OH). ^{13}C NMR ($CDCl_3$, ppm): 15.70 (C-15); 15.80; 17.25; 19.23; 22.62; 27.34; 30.28; 31.11; 31.22; 34.35; 35.35; 36.71; 38.48; 45.00; 52.83; 116.91 (CN); 118.13 (CN); 137.40 (C-4); 141.22 (C-5); 193.24 (C-3). HRMS (TOF) m/z: $C_{20}H_{26}N_2O_2$ $[M+H]^+$ calculated: 327.20670. Found: 327.20652.

4.1.8. 3-Oxo-16,17-secoandrosta-1,4-diene-16,17a-dinitrile (10)

DDQ (0.296 g, 1.32 mmol), TFA (0.02 mL, 0.26 mmol) and BSTFA (0.8 mL, 2.98 mmol) was added to a solution of compound **7** (0.204 g, 0.66 mmol) in dry toluene (9 mL) and refluxed for 6 h under an argon atmosphere. When the reaction was complete, the resulting mixture was washed with saturated sodium hydrogen carbonate until the water layer became visibly yellow. The organic layer was then dried and the solvent removed. Crude product was purified by flash chromatography (toluene–ethyl acetate, 15:1) affording pure compound **10** (91.4 mg, 45%, mp 180 °C after recrystallization from *n*-hexane–ethyl acetate) in the form of white solid.

IR (KBr, cm^{-1}): 2944, 2857, 2243, 1662, 1623, 1604, 755. ^1H NMR ($CDCl_3$, ppm): 1.20 (s, 3H); 1.26 (s, 3H); 6.10 (s, 1H, H-4); 6.26 (dd, 1H, $J_{1,2}$ = 10.4 Hz, $J_{2,4}$ = 1.8 Hz, H-2); 7.03 (d, 1H, J = 10.4 Hz, H-1). ^{13}C NMR ($CDCl_3$, ppm): 16.04 (C-15); 18.78 (C-19); 19.16 (C-18); 21.91; 30.96; 32.12; 32.78; 35.67; 36.91; 38.21; 42.89; 44.76; 50.54; 116.71 (CN); 117.97 (CN); 124.06 (C-4); 128.10 (C-2); 154.10 (C-1); 166.82 (C-5); 185.81 (C-3). HRMS (TOF) m/z: $C_{20}H_{24}N_2O$ $[M+H]^+$ calculated: 309,19614. Found: 309, 19609.

4.2. Antiproliferative activity

4.2.1. Cell lines and cell culture

Six human tumor cell lines (cervical carcinoma, HeLa; breast adenocarcinoma ER−, MDA-MB-231; prostate cancer, PC3; breast adenocarcinoma ER+, MCF-7; colon adenocarcinoma, HT-29; human lung carcinoma, A549) and one human non-cancerous cell

line (normal fetal lung fibroblasts MRC-5), were used in the present study. Cells were grown in Dulbecco's modified Eagle's medium (DMEM) with 4.5% glucose, supplemented with 10% fetal calf serum (FCS, Sigma), antibiotics and antimycotics (Sigma). Cells were cultured in flasks (Costar, 25 cm^2) at 37 °C in 100% humidity with 5% CO_2. Only viable cells, as determined by the trypan blue dye exclusion, were used in subsequent assays.

4.2.2. Measurement of antiproliferative activity using the MTT assay

Compounds were evaluated for antiproliferative activity using the tetrazolium colorimetric MTT assay, after exposure to test compounds for a period of 48 h. Two independent experiments were conducted in quadruplicate for each concentration of test compound (0.001, 0.01, 0.1, 1, 10 and 100 μM). Mean values and standard deviations (SD) were calculated for each concentration. IC_{50} was defined as the dose of compound that inhibits cell growth by 50%. The IC_{50} of each test compound was determined by median effect analysis. The MTT assay is based on cleavage of 3-(4,5-dimethylthiazol-2-yl)-2,5-diphenyl tetrazolium bromide (MTT) to formazan by mitochondrial dehydrogenases in viable cells. Formestan was used as a general control of steroidal cytotoxicity. Doxorubicin was used as a non-specific cytotoxicity control. Exponentially growing cells were harvested, counted by trypan blue exclusion, and plated onto 96-well microtiter plates (Costar) at an optimal seeding density to assure logarithmic growth throughout the assay period. Viable cells were plated at 90 μL per well, and pre-incubated in complete medium at 37 °C for 24 h to ensure cell stabilization prior to addition of test compounds. Test compounds, at 10× the required final concentration, in growth medium (10 μL per well), were added to all wells except controls, and microplates were incubated for 24 h. Wells containing cells without test compounds were used as a control. Three hours before the end of the incubation period, 10 μL of MTT solution was added to each well. MTT was dissolved in medium at 5 mg mL^{-1} and filter sterilized, to remove a small amount of insoluble residue present in some batches of MTT. Acidified 2-propanol (100 mL of 0.04 M HCl in 2-propanol) was added to each well, and mixed thoroughly to dissolve the dark blue crystals. After a few minutes incubation at room temperature (to ensure that all crystals were dissolved), plates were read on a spectrophotometric plate reader (Multiscan MCC340, Labsystems) at 540/690 nm. Wells without cells containing complete medium and MTT only were used as a blank.

4.3. X-ray crystal structure determination of compound 7

X-ray diffraction data for **7** was collected at room temperature on an Oxford Diffraction Gemini S diffractometer with graphite-monochromated MoKα radiation (λ = 0.7107 Å). Data reduction was performed in CrysAlis RED (Oxford Diffraction, UK). Space group determination was based on analysis of Laue class and systematically absent reflections. The structure was solved by direct methods using SIR92, and refined using full-matrix least-squares.[47] Non-hydrogen atoms were refined anisotropically and H atoms were treated by a mixture of independent and constrained refinement. All calculations were performed using SHELXL97, PARST and PLATON, as implemented in WINGX.[48] Crystal data and refinement parameters are summarized in Supplemental S3.

4.4. Molecular docking

4.4.1. Protein (receptor) structural coordinate preparation

Structural coordinates for estrogen receptor α (ERα: PDB ID 1A52), androgen receptor (AR: PDB ID 2AMA), Aromatase (CYP19A1: PDB ID 3EQM) and 17α-hydroxylase/17,20-lyase (CYP17A1: PDB ID 3RUK) were obtained from the protein data bank (http://www.rcsb.org). Coordinates for ligands and water molecules were removed using a text editor. Hydrogen atoms and Gasteiger partial charges were added using the script 'receptor.c' in VEGA ZZ 3.0.1.[49] Non-polar hydrogen atoms were merged in VEGA ZZ and receptor coordinate files saved in PDBQT format for docking simulations.

4.4.2. Ligand structural coordinate preparation

Using the X-ray structure of **7**, 3D structural models of compounds **5**–**7**, **9** and **10** were created in AVOGADRO 1.0.3 (http://avogadro.openmolecules.net/).[26] Hydrogen atoms were added and ligand geometries were optimized (MMFF94 force field: 500 steps of conjugate gradient energy minimization followed by 500 steps of steepest descent energy minimization with a convergence of 10×10^{-7}) in the program AVOGADRO. Non-polar hydrogen atoms were merged and Gasteiger partial charges partial charges were calculated using the script 'ligand.c' in VEGA ZZ 3.0.1 and the resulting ligand coordinate files were saved in PDBQT format. The predicted solubility ($c\log P$) and topological polar surface area/TPSA of compounds **5**–**10** was calculated in ChemBio3D Ultra.

4.4.3. Grid map calculations

Autodock grid maps were calculated for each receptor using AutoGrid 4.[35] Grid maps were centered on ligands present in the original receptor structure files and a grid box of $50 \times 50 \times 50$ was chosen, with a grid spacing of 0.375 Å. Maps were calculated for each atom type in each ligand along with an electrostatic and desolvation map using a dielectric value of −0.1465.

4.4.4. Molecular docking simulations

Initial ligand position, orientation and dihedral offsets were randomized. Torsional degrees of freedom for each ligand were determined in AutoDockTools.[35] Molecular docking simulations used the Larmarckian genetic algorithm, with 2,500,000 energy evaluations and a GA population of 150. Ten hybrid GA-LS runs were performed for each simulation. Results were visualized in PyMol (http://www.pymol.org/) and compared with the X-ray structures of ligand bound receptors: ERα, AR, CYP19A1 and CYP17A1. Autodock and AutoGrid were run remotely at the National Biomedical Computational Resource (http://nbcr-222.ucsd.edu/opal2)[50] using the PyRx virtual screening tool.[34] Control redocking simulations using ligands present in the receptor crystal structures correctly reproduced ligand–protein geometries found in the respective X-ray structures. Based on these controls, predicted binding energies $\leqslant -10.00$ kcal/mol were considered indicative of strong binding.

4.5. Ligand-based virtual screening

4.5.1. ChemMapper3D

Ligand-based 3D similarity searches were conducted on **10** using ChemMapper3D.[37] Compound **10** was screened against the DrugBank database, consisting of 7739 drugs associated with 4283 non-redundant protein targets.[39] Potential protein targets were ranked by ChemMapper3D based on the 3D similarity between **10** and ligands present in the DrugBank database.

4.5.2. Fast molecular docking using idTarget

Ligand-based virtual screening was conducted for **10** using the program idTarget.[42] A 3D structural model of **10** was input and rapid molecular docking was performed against all protein structures in the PDB using MEDock,[42] followed by rescoring using an Autodock4 scoring function.[35] An idTarget *Z*-score is also reported which attempts to model the affinity profile of each binding site. Proteins were considered to be possible ligand targets if the idTar-

get binding energy was stronger than −9.5 kcal/mol with a *Z*-score was 1.0 or better. This preliminary list was filtered using published lists of proteins expressed in hormone-dependent and independent breast cancer cells.

Acknowledgments

We thank the Ministry of Education, Science and Technological Development of the Republic of Serbia for financial support (Grant No. 172021).

Supplementary data

Supplementary data associated with this article can be found, in the online version, at http://dx.doi.org/10.1016/j.bmc.2014.12.069.

References and notes

1. Gupta, A.; Kumar, B. S.; Negi, A. S. *J. Steroid Biochem. Mol. Biol.* **2013**, *137*, 242.
2. Siegfried, J. M.; Stabile, L. P. *Semin. Oncol.* **2014**, *41*, 5.
3. Patani, N.; Martin, L. A. *Mol. Cell. Endocrinol.* **2014**, *382*, 683.
4. Vis, A. N.; Schroder, F. H. *BJU Int.* **2009**, *104*, 1191.
5. Vis, A. N.; Schroder, F. H. *BJU Int.* **2009**, *104*, 438.
6. Folkerd, E. J.; Dowsett, M. *J. Clin. Oncol.* **2010**, *28*, 4038.
7. Ghosh, D.; Griswold, J.; Erman, M.; Pangborn, W. *Nature* **2009**, *457*, 219.
8. Maurelli, S.; Chiesa, M.; Giamello, E.; Di Nardo, G.; Ferrero, V. E.; Gilardi, G.; Van Doorslaer, S. *Chem. Commun. (Camb.)* **2011**, *47*, 10737.
9. DeVore, N. M.; Scott, E. E. *Nature* **2012**, *482*, 116.
10. Valachis, A.; Mauri, D.; Polyzos, N. P.; Mavroudis, D.; Georgoulias, V.; Casazza, G. *Crit. Rev. Oncol. Hematol.* **2010**, *73*, 220.
11. Anderson, J. *BJU Int.* **2003**, *91*, 455.
12. Bines, J.; Dienstmann, R.; Obadia, R. M.; Branco, L. G.; Quintella, D. C.; Castro, T. M.; Camacho, P. G.; Soares, F. A.; Costa, M. E. *Ann. Oncol.* **2014**, *25*, 831.
13. Schiavon, G.; Smith, I. E. *Breast Cancer Res.* **2014**, *16*, 206.
14. Chumsri, S.; Howes, T.; Bao, T.; Sabnis, G.; Brodie, A. *J. Steroid Biochem. Mol. Biol.* **2011**, *125*, 13.
15. Ziauddin, M. F.; Hua, D.; Tang, S. C. *Cancer Metastasis Rev.* **2014**, *33*, 791.
16. Fleming, F. F.; Yao, L.; Ravikumar, P. C.; Funk, L.; Shook, B. C. *J. Med. Chem.* **2010**, *53*, 7902.
17. Teno, N.; Miyake, T.; Ehara, T.; Irie, O.; Sakaki, J.; Ohmori, O.; Gunji, H.; Matsuura, N.; Masuya, K.; Hitomi, Y.; Nonomura, K.; Horiuchi, M.; Gohda, K.; Iwasaki, A.; Umemura, I.; Tada, S.; Kometani, M.; Iwasaki, G.; Cowan-Jacob, S. W.; Missbach, M.; Lattmann, R.; Betschart, C. *Bioorg. Med. Chem. Lett.* **2007**, *17*, 6096.
18. Thomas, J. L.; Bucholtz, K. M.; Sun, J.; Mack, V. L.; Kacsoh, B. *Mol. Cell. Endocrinol.* **2009**, *301*, 174.
19. Djurendić, E. A.; Sakač, M. N.; Zaviš, M. P.; Gaković, A. R.; Čanadi, J. J.; Andrić, S. A.; Klisurić, O. R.; Kojić, V. V.; Bogdanović, G. M.; Gaši, K. M. *Steroids* **2008**, *73*, 681.
20. Sakač, M.; Gaković, A.; Stojanović, S.; Djurendić, E.; Kojić, V.; Bogdanović, G.; Gaši, K. P. *Bioorg. Chem.* **2008**, *36*, 128.
21. Djurendić, E. A.; Zaviš, M. P.; Sakač, M. N.; Čanadi, J. J.; Kojić, V. V.; Bogdanović, G. M.; Penov Gaši, K. M. *Steroids* **2009**, *74*, 983.
22. Yadav, M. R.; Sabale, P. M.; Giridhar, R.; Zimmer, C.; Hartmann, R. W. *Steroids* **2012**, *77*, 850.
23. Leese, M. P.; Jourdan, F. L.; Gaukroger, K.; Mahon, M. F.; Newman, S. P.; Foster, P. A.; Stengel, C.; Regis-Lydi, S.; Ferrandis, E.; Di Fiore, A.; De Simone, G.; Supuran, C. T.; Purohit, A.; Reed, M. J.; Potter, B. V. *J. Med. Chem.* **2008**, *51*, 1295.
24. Lavecchia, A.; Di Giovanni, C. *Curr. Med. Chem.* **2013**, *20*, 2839.
25. Marcos-Escribano, A.; Bermejo, F. A.; Bonde-Larsen, A. L.; Retuerto, J. I.; Sierra, I. H. *Tetrahedron* **2009**, 65.
26. Hanwell, M. D.; Curtis, D. E.; Lonie, D. C.; Vandermeersch, T.; Zurek, E.; Hutchison, G. R. *J. Cheminf.* **2012**, *4*, 17.
27. Ertl, P.; Rohde, B.; Selzer, P. *J. Med. Chem.* **2000**, *43*, 3714.
28. Ajduković, J. J.; Djurendić, E. A.; Petri, E. T.; Klisurić, O. R.; Ćelić, A. S.; Sakač, M. N.; Jakimov, D. S.; Gaši, K. M. *Bioorg. Med. Chem.* **2013**, *21*, 7257.
29. David-Beabes, G. L.; Overman, M. J.; Petrofski, J. A.; Campbell, P. A.; de Marzo, A. M.; Nelson, W. G. *Int. J. Oncol.* **2000**, *17*, 1077.
30. Zoppi, S.; Lechuga, M.; Motta, M. *J. Steroid Biochem. Mol. Biol.* **1992**, *42*, 509.
31. Jordan, V. C.; Brodie, A. M. *Steroids* **2007**, *72*, 7.
32. Tanenbaum, D. M.; Wang, Y.; Williams, S. P.; Sigler, P. B. *Proc. Natl. Acad. Sci. U.S.A.* **1998**, *95*, 5998.
33. Pereira de Jesus-Tran, K.; Cote, P. L.; Cantin, L.; Blanchet, J.; Labrie, F.; Breton, R. *Protein Sci.* **2006**, *15*, 987.
34. Wolf, L. K. *Chem. Eng. News* **2009**, *87*, 31.
35. Morris, G. M.; Huey, R.; Lindstrom, W.; Sanner, M. F.; Belew, R. K.; Goodsell, D. S.; Olson, A. J. *J. Comput. Chem.* **2009**, *30*, 2785.
36. Woo, L. W.; Bubert, C.; Purohit, A.; Potter, B. V. *ACS Med. Chem. Lett.* **2011**, *2*, 243.
37. Gong, J.; Cai, C.; Liu, X.; Ku, X.; Jiang, H.; Gao, D.; Li, H. *Bioinformatics* **1827**, *2013*, 29.
38. Law, V.; Knox, C.; Djoumbou, Y.; Jewison, T.; Guo, A. C.; Liu, Y.; Maciejewski, A.; Arndt, D.; Wilson, M.; Neveu, V.; Tang, A.; Gabriel, G.; Ly, C.; Adamjee, S.; Dame, Z. T.; Han, B.; Zhou, Y.; Wishart, D. S. *Nucleic Acids Res.* **2014**, *42*, D1091.
39. Wishart, D. S.; Knox, C.; Guo, A. C.; Shrivastava, S.; Hassanali, M.; Stothard, P.; Chang, Z.; Woolsey, J. *Nucleic Acids Res.* **2006**, *34*, D668.
40. Penning, T. M.; Byrns, M. C. *Ann. N. Y. Acad. Sci.* **2009**, *1155*, 33.
41. Endo, S.; Hu, D.; Matsunaga, T.; Otsuji, Y.; El-Kabbani, O.; Kandeel, M.; Ikari, A.; Hara, A.; Kitade, Y.; Toyooka, N. *Bioorg. Med. Chem.* **2014**, *22*, 5220.
42. Wang, J. C.; Chu, P. Y.; Chen, C. M.; Lin, J. H. *Nucleic Acids Res.* **2012**, *40*, W393.
43. Gruvberger-Saal, S. K.; Bendahl, P. O.; Saal, L. H.; Laakso, M.; Hegardt, C.; Eden, P.; Peterson, C.; Malmstrom, P.; Isola, J.; Borg, A.; Ferno, M. *Clin. Cancer Res.* **1987**, *2007*, 13.
44. Skliris, G. P.; Leygue, E.; Watson, P. H.; Murphy, L. C. *J. Steroid Biochem. Mol. Biol.* **2008**, *109*, 1.
45. Manas, E. S.; Unwalla, R. J.; Xu, Z. B.; Malamas, M. S.; Miller, C. P.; Harris, H. A.; Hsiao, C.; Akopian, T.; Hum, W. T.; Malakian, K.; Wolfrom, S.; Bapat, A.; Bhat, R. A.; Stahl, M. L.; Somers, W. S.; Alvarez, J. C. *J. Am. Chem. Soc.* **2004**, *126*, 15106.
46. Brozic, P.; Turk, S.; Rizner, T. L.; Gobec, S. *Curr. Med. Chem.* **2011**, *18*, 2554.
47. Altomare, A.; Burla, M. C.; Cavalli, M.; Cascarano, G.; Giacovazzo, C.; Gagliardi, A.; Moliterni, A. G.; Polidori, G.; Spagna, R. *J. Appl. Crystallogr.* **1999**, *32*, 115.
48. Farrugia, L. J. *J. Appl. Crystallogr.* **1999**, *32*, 837.
49. Pedretti, A.; Villa, L.; Vistoli, G. *j. Comput. Aided Mol. Des.* **2004**, *18*, 167.
50. Ren, J.; Williams, N.; Clementi, L.; Krishnan, S.; Li, W. W. *Nucleic Acids Res.* **2010**, *38*, W724.